Proceedings of IMECE09:
2009 ASME International Mechanical Engineering Congress and Exposition
November 13-19, 2009, Lake Buena Vista, Florida, USA

IMECE2009-13077

REGENERATIVE BRAKING POTENTIAL AND ENERGY SIMULATIONS FOR A PLUG-IN HYBRID ELECTRIC VEHICLE UNDER REAL DRIVING CONDITIONS

LASB Martins
School of Engineering, University of Minho
4800-058 Guimarães, Portugal
lmartins@dem.uminho.pt

JMO Brito
School of Engineering, University of Minho
4800-058 Guimarães, Portugal
jorgemobrito@gmail.com

AMD Rocha
School of Engineering, University of Minho
4800-058 Guimarães, Portugal
alberto38090@gmail.com

JJG Martins
School of Engineering, University of Minho
4800-058 Guimarães, Portugal
jmartins@dem.uminho.pt

ABSTRACT

There are several possible configurations and technologies for the powertrains of electric and hybrid vehicles, but most of them will include advanced energy storage systems comprising batteries and ultra-capacitors. Thus, it will be of capital importance to evaluate the power and energy involved in braking and the fraction that has the possibility of being regenerated. The Series type Plug-in Hybrid Electric Vehicle (S-PHEV), with electric traction and a small Internal Combustion Engine ICE) powering a generator, is likely to become a configuration winner. The first part of this work describes the model used for the quantification of the energy flows of a vehicle, following a particular route. Normalised driving-cycles used in Europe and USA and real routes and traffic conditions were tested. The results show that, in severe urban driving-cycles, the braking energy can represent more than 70% of the required useful motor-energy. This figure is reduced to 40% in suburban routes and to a much lower 18% on motorway conditions. The second part of the work consists on the integration of the main energy components of an S-PHEV into the mathematical model. Their performance and capacity characteristics are described and some simulation results presented. In the case of suburban driving, 90% of the electrical motor-energy is supplied by the battery and ultra-capacitors and 10% by the auxiliary ICE generator, while on motorway these we got 65% and 35%, respectively. The simulations also indicate an electric consumption of 120 W.h/km for a small 1 ton car on a suburban route. This value increases by 11% in the absence of ultra-capacitors and a further 28% without regenerative braking.

NOMENCLATURE

a	acceleration	[m.s^{-2}]
A_F	frontal area	[m^2]
C_D	aerodynamic drag coefficient	[-]
CC_α	Cornering coefficient	[-]
D-class	average large-family European car	
E	Energy, generic	[W.h]
e	specific energy, generic	[W.h/km]
F	Force, generic	[N]
g	gravity	[m.s^{-2}]
LLFCC	Light Low-Friction City-Car	
m	Vehicle mass	[kg]
Mot	Motorway route	
NR	National Road – suburban route	
T	Torque	[N.m]
RRC	quasi-static tyre rolling resistance coefficient	[-]
S	longitudinal slip ratio	[-]
SOC	state of charge	
S-PHEV	Series Plug-in Hybrid Electric Vehicle	
TTW	Tank-To-Wheel	
u	vehicle speed	[m.s^{-1}]
UC	Ultra Capacitors	
W	vehicle weight	[N]
WTT	Well-To-Tank	
WTW	Well-To-Wheel	

Greek Symbols

α	Slip angle	[rad]
ρ	density	[kg.m^{-3}]

θ	road slope	[rad]
Ω	angular velocity	[rad.s^{-1}]

Subscripts

A	total friction
DRAG	aerodynamic drag
GRAD	road slope
i	generic variable
M	motor
R1	free rolling resistance
R2	fictitious resistance due to longitudinal slip
RY	rolling resistance due to cornering
T	total
X	longitudinal direction of travel
Y	lateral direction
Z	normal direction

1 INTRODUCTION

From the energy manager and the environmentalist points of view, the most important characteristic of any energy system is the efficient use of primary energy i.e., in the case of an automobile, the Well-to-Wheel (WTW) analysis in terms of total energy use (efficiency), but also of fossil energy use and greenhouse gas emissions, if a meaningful comparison of different vehicle/fuel technologies is to be accomplished. The WTW combines the analyses of the Well-to-Tank (WTT) fuel pathways and of the Tank-to-Wheel efficiency (TTW). For the average gasoline car the WTW efficiency is only about 12 to 15 percent, due to poor engine efficiency and despite low WTT energy losses [1]. On the contrary, the battery-electric car (EV) has the highest TTW efficiency but the WTT losses of producing and distributing electricity are usually very high, yet leading to a WTW efficiency in excess of 21 %, with electricity produced in a thermal power plant [2]. A more recent study by Tesla motors suggests that their new battery-electric prototype will double the WTW efficiency of the Toyota Prius [3]. As Electricity WTT losses strongly depend on the electric generation mix, the numbers can be significantly higher in countries with large electricity production from renewable sources.

There is a lot of controversy about the WTW efficiency of Fuel Cells Vehicles (FCV) but it is usually accepted that it will vary significantly with the pathways used to produce hydrogen. One of the studies estimates values between 13 and 27% [2]. The same study suggests that future diesel and compressed natural gas hybrids could achieve 30 to 32 %. Furthermore, a report by the MIT´s Laboratory for Energy and the Environment [4] concluded, “Even with aggressive research, the hydrogen vehicle will not be better than the diesel HEV in terms of total energy use and greenhouse gas emission by 2020 (...) Also, hybrid concepts allow the recovery of energy dissipated in braking. Thus, in each case the hybrid vehicle is more efficient than its non-hybrid counterpart.”

No information exists about Plug-in Hybrid Electric Vehicles (PHEV), but it is expected that their WTW efficiencies will rang between those of battery-electric (EV) and hybrid-electric (HEV) vehicles. This looks very promising, as PHEV’s do not have the main disadvantages of all-electric cars: poor range and excessive weight. Furthermore, by comparison with a HEV, the use of electricity from the grid will cost 3 to 6 times less than the corresponding gasoline, in the USA and in Europe.

The escalades in the price of fossil fuels lead to the sudden appeal of hybrid cars, as confirmed by the sales success of the models available in the USA and in Europe. This attractiveness will be deeper in the future, mainly due to further restrictions in CO2 emissions. Yet, with the HEV models currently available in the market, the traction of the car is mainly done by the large engine with only a modest contribution from the electric motor/generator, and the battery system is undersized both in capacity and peak power. The consequences are plenty: plug-in is not possible, the engine frequently runs in low charge/efficiency conditions; most of the kinetic energy is wasted during the regenerative braking, leading to overall poor energy efficiency, despite sophisticated transmissions and complex control/management systems. For example, the Honda Insight is still the most “electric” of all, yet it has a 50 kW gasoline engine for a nominal 10 kW electric motor but, in reality, this motor never exceeds 6.5 kW as a motor and 8~9 kW as a generator [5]. The nominal battery capacity is merely 0.94 kWh but the charge and discharge limits define a usable capacity of barely 58% of the nominal value. A worse scenario happens with both the Honda Civic Hybrid and the Prius: only about 35% of the battery 1 kWh nominal capacity is effectively used. Also, according to a Swedish study [6], the planetary gear transmission of the Prius is inefficient because during acceleration, the excess engine power must pass two electric motors (a generator and a motor) and two semiconductor inverters before reaching the tyre. The engine to motor disproportion is even bigger with the very powerful V6 engines of the new SUV and luxury HEV models that recently came to the market. All these cars are costly to produce and take little advantage of the hybrid philosophy.

The likely evolution will be plug-in hybrid vehicles where the batteries can be recharged from the electricity grid. This will require a significant boost to their capacity, even though, to figures much inferior to those needed for all-electric cars (>20 kWh/ton). In the near future, “plug-in hybrids” offer the best opportunity to reduce the fossil-fuel dependence of the transportation sector, without the need of new infrastructures and with the basic technology already available today. Thus, several organisations and energy experts [7, 8 and 9] suggest that government policies should encourage research and demonstration projects, much needed to bring plug-in versions to the market.

The final objective of this project is to simulate the operation of a small Plug-in Hybrid Electric Vehicle (PHEV) that will include an advanced energy storage system and thus help in the design of a prototype powertrain. The vehicle will be of the “Series” type (S-PHEV), working with only-electric drive, and will be assisted by a small gasoline ICE coupled to

an electric generator and complemented by a battery and ultra-capacitors. The storage of energy in these two types of components will be made in several ways: recharge from the grid, small ICE-generator, and regenerative braking by the use of the powerful electric motor as a generator. The ultra-capacitors will deliver high peak power both during strong acceleration (discharge) and vigorous braking (charge), thus improving the efficiency and protecting the battery. As a concept, an S-PHEV will be more an electric vehicle with the possibility of recharging the battery by a small combustion engine always working at the maximum efficiency point, than a car with its large gasoline engine assisted by an electric motor and a battery. By initializing the drive with a fully loaded battery, the vehicle should be able to run for 40 to 60 km in full-electric mode with no consumption of gasoline. Afterwards the engine-generator will start, thus guaranteeing a driving range only limited by the fuel-tank capacity. Such a car will be mechanically simpler than the usual hybrids, a match to lower production costs.

In order to simulate the operation of a vehicle along any real route, a physical model was developed and a code written in the MatLab/Symulink environment, described in the next section. The real route data was obtained via a dedicated GPS system briefly portrayed in section 3 and the simulation results are presented in section 4.

2 MATHEMATICAL MODEL

The coordinate system adopted by SAE International [10] for tyre analysis is shown in Fig.1. A similar one is used in this work for vehicle analysis but with the origin coincident with the vehicle's centre of mass. For the sake of simplicity, the inclination angle γ and the overturning moment M_x are both neglected: this corresponds to a two-wheel model where the forces acting on the left wheels are considered equal to the ones acting on the matching right wheel (but different for front and rear wheels).

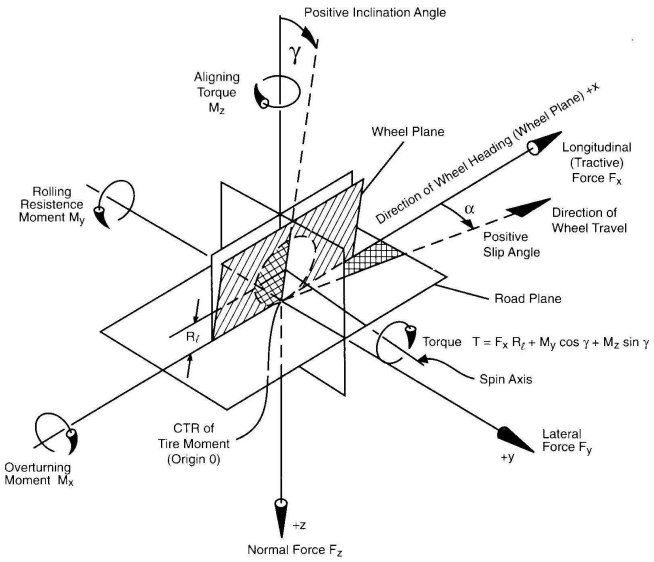

FIGURE 1 – Tyre coordinate system according to SAE[10]

To evaluate the power and energy flows involved in the run of the car it is necessary to know the relevant instantaneous forces in the direction of travel. The total force F_T that is responsible for the vehicle longitudinal acceleration a_x is given by:

$$F_T = m \times a_X = F_X - F_A - F_{GRADE} \quad (1)$$

where m is the mass of the car, F_X is the traction force that pushes the vehicle, exerted by the road on the traction tyres, (negative when braking and for all tyres), F_A is the sum of all the friction forces (basically rolling resistance and drag) and F_{GRADE} is the weight component in the longitudinal direction, cause by the slope of the road,

$$F_{GRADE} = W \cdot \sin(\theta) = m \cdot g \cdot \sin(\theta) \quad (2)$$

According to Gillespie [11], if the vehicle is not turning and excluding drag, the main forces acting on it can be represented as in Fig. 2.

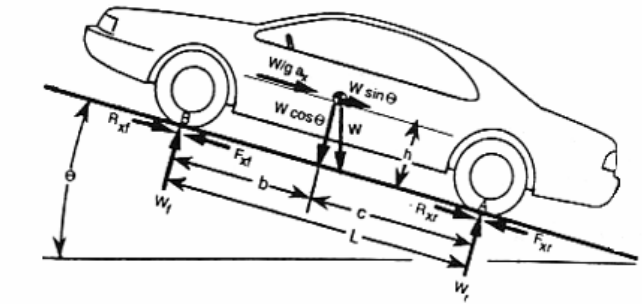

FIGURE 2 – Forces acting on a generic vehicle and their location (excluding drag)

The drag force F_{DRAG} depends on vehicle frontal area A_F, air density ρ_{air}, drag coefficient C_D and vehicle velocity u [12],

$$F_{DRAG} = \frac{1}{2} \cdot \rho_{air} \cdot C_D \cdot A_F \cdot u^2 \quad (3)$$

The tyre rolling resistance force F_R represents an important part of F_A, particularly at low velocities when drag is low [11] but the latter predominates at high speeds. For each wheel F_R is the sum of three components,

$$F_R = F_{R1} + F_{R2} + F_{RY} \quad (4)$$

where F_{R1} is the free or coasting rolling resistance, F_{R2} is the additional resistance due to longitudinal slip (when the wheel is submitted to a traction or braking force) and F_{RY} arises when the car is cornering.

The free rolling resistance F_{R1} occurs when there is no motor or braking torque applied to the vehicle wheels, that is the longitudinal traction or braking force F_X is zero and can be calculated for the whole car by [11] ,

$$F_{R1} = RRC \cdot \left(1 + \frac{3{,}6 \cdot u}{161}\right) \cdot W \cdot \cos\alpha \quad (5)$$

provided that the 4 tyres are equal as RRC is the quasi-static tyre rolling resistance coefficient ($u \approx 0$) an W is the car weight. The equation is valid for speeds up to *120 km/h*.

To calculate F_{R2} one needs to know the longitudinal slip ratio defined as,

$$S = \frac{\Omega \cdot R_e}{u} - 1 \quad (6)$$

where Ω is the wheel angular speed and R_e is the effective radius. In the present work the slip ratio S was assumed to vary linearly with the traction or braking force F_X divided by the dynamic vertical load upon the tyre W_Z,

$$S = K \cdot \frac{F_X}{W_Z} \quad (7)$$

and this leads to,

$$F_{R2} = K \cdot \frac{F_X^2}{W_Z} \quad (8)$$

F_{R2} can be considered as a fictitious force matching the dissipated power associated to the longitudinal slip (equal to wheel torque multiplied by the angular slip velocity). The slope constant K was considered equal to 0.15, corresponding to a reference slip ratio of 15% and a max. deceleration of 1.0g before *ABS* intervention limit.

With regard to F_{RY}, it is a function of the lateral force F_Y (imposed by the lateral acceleration a_Y of the vehicle when cornering) and of the tyre slip-angle α defined in Fig. 3,

$$F_{RY} = F_Y \cdot \sin\alpha \quad (9)$$

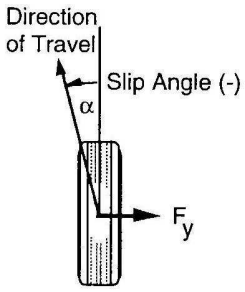

FIGURE 3 – Definition of slip angle α [11].

Again, a linear relationship can be established between the lateral to vertical force ratio and the slip-angle,

$$\frac{F_Y}{F_Z} = CC_\alpha \cdot \alpha \quad (10)$$

for values up to 5 degrees. The slope constant CC_α is called cornering stiffness coefficient and a value of 0.2 deg^{-1} was assumed.

Finally, F_X can be calculated from,

$$F_X = F_T + F_{DRAG} + F_{R1} + F_{RY} \quad (11)$$

and the useful motor force F_M must include the fictitious force F_{R2} , that is to say,

$$F_M = F_X + K \cdot \frac{F_X}{W_Z} \quad (12)$$

The computer program was implemented in MatLab-Simulink with the objective of determining all the relevant energies for a generic car following a predefined route, e.g. the total useful energy that the motor must deliver to the wheels (motor energy), the energy spent on friction (rolling friction; drag), the wasted braking energy, the grade energy (if the initial and final altitudes are different), and so forth.

The route or driving cycle definition comprised the input of the following 3 variables as discrete time series with regular time intervals of 0.2 seconds:

- Vehicle speed u [$m.s^{-1}$];
- Altitude [m];
- Lateral acceleration a_Y [$m.s^{-2}$].

with a linear function describing each variable within each time interval. From these functions all the relevant quantities were calculated namely, the distance travelled by the vehicle between times t_1 an t_2,

$$L_{t1 \to t2} = \int_{t_1}^{t_2} u(t)\, dt \quad (13)$$

the longitudinal acceleration $a_X(t)$,

$$a_X(t) = \frac{du(t)}{dt} \quad (14)$$

a generic force $F_i(t)$, where i stands for any of the forces described above. The corresponding power $P_i(t)$ can be obtained from,

$$P_i(t) = F_i(t) \cdot u(t) \quad (15)$$

and ultimately, the resultant energy flow can be obtained by integration,

$$E_i = \int_{t_1}^{t_2} P_i(t)\, dt \quad (16)$$

Further details about this model can be found in the work of Brito [13].

3 DATA ACQUISITION SYSTEM

In order to obtain data for the dynamic evolution of a car on a real road, a dedicated GPS system and software from MAxQData (model MQGPS) was used. The interface between the unit and a PDA was accomplished via a Bluetooth protocol at a *5Hz* data rate. Even though many variables were available from the resident software, such as longitudinal acceleration, integrated distance, curvature radius, etc, only the above mentioned three variables were use as input for the mathematical model.

GPS systems have inherent errors and in the current application they mainly translate into velocity spurious oscillations and altitude errors. These lead to an artificial increase in both the motor and braking energies that is to a systematic positive error. Thus, the recorded data was imported to an Excel worksheet-file for data filtering before being used in the mathematical model. The filtering process comprised three stages: first, data points with unrealistically longitudinal accelerations were rejected (i.e. with a_x<*-1.0g* when braking or a_x>*+0.6g* when accelerating), then a five point average was made for the velocity data series and finally a 21 point average for the altitude data series.

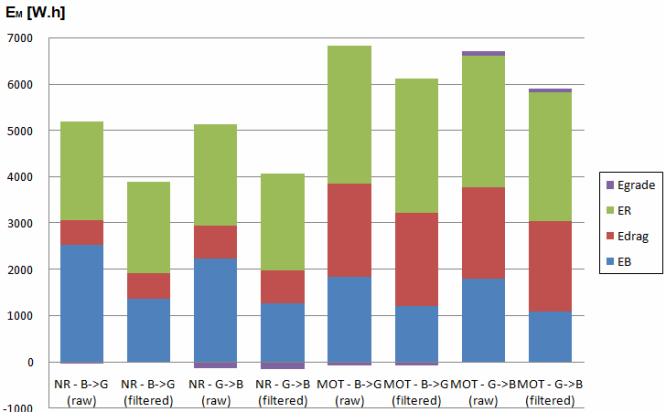

FIGURE 4 – Energy balances: comparison between raw and filtered data; simulation of D-class car on national road and motorway routes; a full column represents the useful motor energy E_M

A comparison between the results of the required energies for 4 simulations, before (raw data) and after data filtering, is shown in Fig.4. Two road routes were used, connecting the cities of Braga and Guimarães and returns, one via a two-lane national road (mainly suburban traffic, *22.8km* length) the other with a motorway profile along *65%* of the *27.5km* distance. With both routes the altitude varied from a minimum of about *110m* to a maximum of *300 m*. An European D-class car was used to record the route data. The results indicate a reduction of about *23%* and *11%* in the required useful motor energies, for the national road and motorway routes, respectively. After filtering and based on data taken from several tests with the car in coasting conditions, it was estimated that the uncertainty of the results for the useful motor energy was about 18 and 11 W.h/km (or 10.7 and 5.1%), again for national road and motorway routes. Further details about the GPS system, routes and data correction procedures can be found in the work of Rocha [14].

4 RESULTS AND DISCUSSION

Two different vehicles were used in the present simulations whose generic friction characteristics are presented in table 1.

TABLE 1 – Characteristics of the studied vehicles

	Light Low Friction City Car (LLFCC)	Conventional Low C_D European D-Class
m [kg]	1000	1600
A_f [m^2]	1.98	2.12
C_D	0.32	0.28
RRC	0.007	0.013

The first one is designated as Light Low Friction Car (LLFCC) and has the ideal characteristics for urban and suburban operation and to the future implementation of a S-PHEV powertrain. The second corresponds to the car used to collect the data and to the average large-family (D-class)

European car, with excellent aerodynamics but high performance tyres (high RRC).

Model application to normalised driving cycles

The application of the mathematical model to the normalised driving cycles was straightforward, as no experimental data was needed and only the velocity time series was required: the altitude and lateral acceleration were zero. The analysed driving Cycles were: The European Elementary Urban Cycle (ECE 15, the European Extra Urban Driving Cycle (EUDC), the EPA Federal Test Procedure (FTP 75), the Highway Fuel Economy Test driving schedule (HWFET), the unified dynamometer driving schedule (LA92), the New York City Cycle (NYCC) and the supplemental FTP driving schedule (US06).

The results for the specific motor energy e_M (W.h/km), broken up in the different friction energies e_{R1}, e_{R2}, e_{DRAG} and e_{BRAKE}, are presented in Fig.5 for the D-class vehicle and in Fig.6 for the small LLFCC.

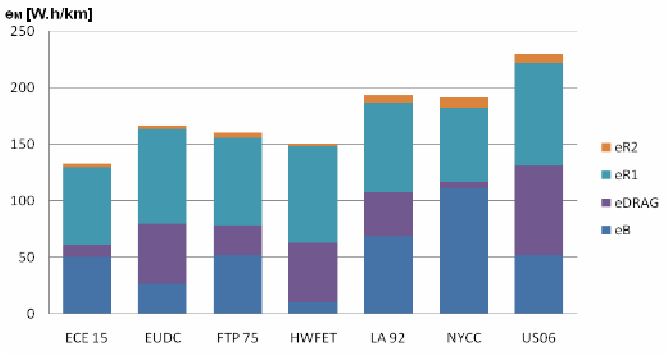

FIGURE 5 – Specific energies for the D-class vehicle undergoing various normalised cycles; a full column is e_M.

In Fig.6 the braking energy e_{BRAKE} is separated in regenerative energy (e_{B_R}) and dissipated mechanical or hydraulic energy (e_{B_H}), by assuming that the car has a regenerative braking system but with a power limited to 8 kW.

It can be observed that: for each vehicle and all driving schedules, the free rolling resistance energy e_{R1} is fairly constant and significantly lower in the case of the LLFCC due the low weight and low friction tyres (RRC); the dissipated energy due to longitudinal slip e_{R2} is always small but increases in the more aggressive schedules such as the NYCC and the US06; the dissipated energy due to aerodynamic drag e_{DRAG} varies notably and is at maximum in the high speed schedules (US06, HWFET and EUDC) and almost negligible in the urban driving cycles (NYCC and ECE 15); the braking energy e_{BRAKE} also varies significantly with the type of schedule and the highest specific value occurs in the NYCC (representing 70% of the motor energy) followed by the mixed and aggressive LA92. The lowest value occurs in the soft motorway HWFET schedule, equivalent to only 8% of the motor energy.

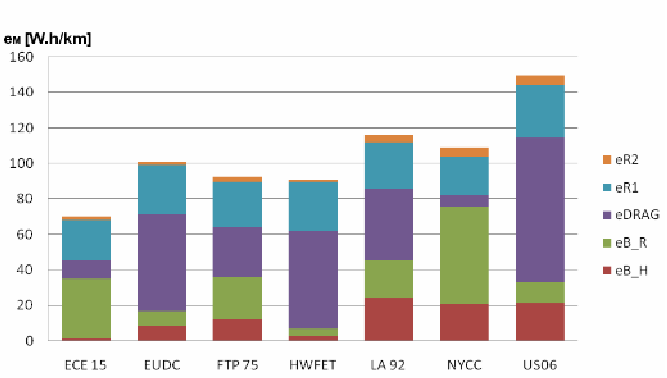

FIGURE 6 – Specific energies for the 1 ton vehicle (LLFCC) undergoing various driving cycles with regenerative braking power limited to 8 kW

It is important to note that the quota of the braking energy increases when the friction characteristics of the vehicle decrease, hence raising the potential for regenerative braking.. Also, the separation of the braking energy into regenerative and mechanically dissipated (in the hydraulic brakes), gives interesting indications: a higher proportion of dissipated braking reveals an aggressive schedule with powerful decelerations, like the US06 and the LA92. Thus, from Fig.6 it can be concluded that both European schedules are soft and non-realistic, very far from present day traffic conditions.

Model application to real road traffic data

The mathematical model was applied to real traffic data. The routes and data acquisition system were described in section 3. The results indicate that the braking energy was about 34% of the motor energy for the national road path and only 19% for the motorway route for the D-class vehicle (filtered results of Fig.4). The corresponding values for the LLFCC were 40% and 18%: the higher value for the national road, in comparison with the D-class car, was expected as the vehicle has lower rolling resistance and the value for the motorway route can be explained by the poorer aerodynamics that offsets the lower friction at high speeds. In real route schedules there are two new factors that influence the energy flows of a vehicle and are absent in the normalised cycles: the friction energy due to cornering E_{RY} and the altitude variations. E_{RY} was found to vary from 2.9% on motorway to 3.7% on the national road of the respective motor energies. This factor tends decrease the energy braking potential (even this is controversial as a highly sinuous road leads to a more aggressive drive) but altitude variations do the opposite. The latter effect appears to be predominantly and so real routes have a larger energy braking potential than do “equivalent” normalised schedules.

The model was then complemented with the introduction of the main powertrain components of a S-PHEV, namely: the battery, ultra-capacitors, reversible electric motor-generator and auxiliary Internal Combustion Engine and generator (ICE-

generator). The main characteristics of these components for the two studied vehicles are presented in table 2.

TABLE 2 – Components Characteristics of the two vehicles simulated as PHEV's

	Light LF City Car	European D-class
Electric rev. motor/gen.	30 kW	53 kW
Battery capacity	7.1 kW.h	11.0 kW.h
Battery power (η= 90%)	13.4 kW	20 kW
UC capacity	65 W.h	100 W.h
ICE-generator	6.5 kW	10 kW

In order to properly simulate the energy inflows and outflows of these components their efficiencies need to be taken into account: the values are summarised in table 3. For the reversible electric motor, a manufacturer efficiency map was considered that was converted into a MatLab double-entry table (efficiency as a function of torque and motor speed). As for the battery a mathematical function was defined for the charging operation and another for the discharge depending on load. A constant efficiency of 95% was assumed for the ultra-capacitors in both charge and discharge operation.

TABLE 3 – Efficiencies used in the simulations of the powertrain components

	Efficiency η
Electric revers. motor/gener.	manufacturer efficiency map
Battery charge/discharge	Functions of load
Battery charge from grid	95%
Ultra-capacitors	95%
ICE-generator	35% (ICE) ; 90% (generator)

An operational strategy was defined, giving priority to battery use in low-power situations and to UC use when higher powers were needed: whenever the battery efficiency would be less than 90% the excess power was dealt by the UC. Thus, the battery could be protected and the overall efficiency of the system improved. If the UC state of charge was below 10% of full charge, the ICE-generator would start.

By running the code with a particular route as input, the state o the different energy components could be evaluated along the evolution of time and the relevant energies integrated. As an example, Fig.5 presents the Ultra-capacitors State Of Charge (SOC) evolution versus road altitude, for one o the simulations, in this case the D-class vehicle along the national suburban route.

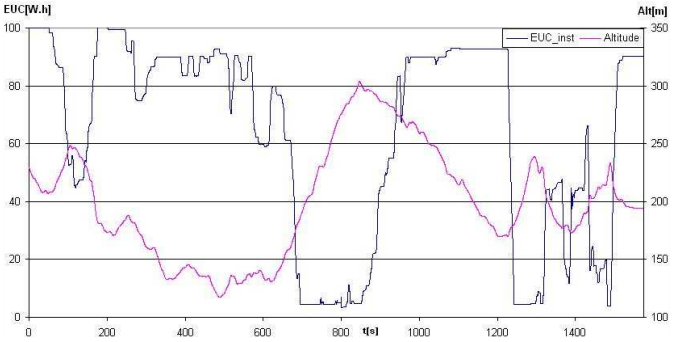

Figure 7 – Simulated Ultra-Capacitors SOC evolution for the D-class vehicle, along the national suburban route; road altitude also presented.

Fig.8 shows the simulated operation points of the reversible electric motor-generator, for the small low friction vehicle along the national suburban road: the 30 kW motor is capable o handling all the operating points and the large majority of them is within the continuous power limit of 20 kW.

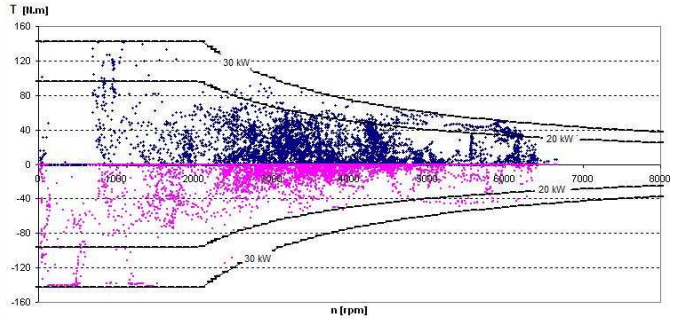

Figure 8 – Simulated motor/generator operation points, for the small LLFCC vehicle on the national suburban route.

For the stipulated operational strategy, 90% of motor consumed electricity is supplied by the battery and 10% by the auxiliary IC-generator, while on motorway these numbers change to 65 and 35%, respectively.

Finally, in Fig.9 a comparison is made for the consumed grid-electricity for the two vehicles simulated in "all-electric mode" (that is with the ICE-generator always off), suburban traffic and with three possible powertrain configurations: (i) battery plus UC; (ii) only battery; (iii) only battery and without regenerative braking. Without the UC, electricity consumption increases buy 11% and without regenerative braking a further 28%. It should be noted that with the configurations (ii) and (iii), the battery would have to handle all the peak-power situations with a shortened life as consequence.

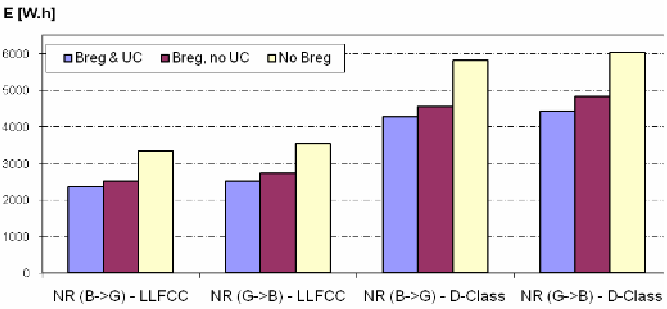

Figure 9 – Comparison of electricity consumption for the two vehicles along the national suburban route, with and without Ultra-Capacitors and without regenerative braking

CONCLUSIONS

In this study, a mathematical model was developed to simulate all the relevant energy flows involved in a vehicle following a pre-defined route. The model was applied to normalised driving cycles and to real-traffic data obtained via a GPS dedicated system. The simulation results indicate that the software can be an important tool in the powertrain development for a plug-in hybrid electric vehicle, namely in the design, component sizing and in the definition of operational strategies. In addition, the following conclusions may be drawn:

Normalised driving schedules are inadequate to properly evaluate the regenerative braking potential of hybrid vehicles, as they do not take into account cornering friction and road slopes. Some of the schedules are too simple to represent present day aggressive traffic conditions.

The GPS-based data acquisition system gave reasonable results, but accuracy can be significantly improved with the introduction of accelerometer sensors and a barometric altimeter.

The braking energy potential varies notably with the road driving schedules and is the greatest for urban traffic and the least for motorway conditions. For real suburban traffic the simulations indicated a braking energy potential of 40% of the useful motor energy. The potential is higher for low friction vehicles.

The use of ultra-capacitors in parallel with the battery, even with a low specific capacity of 65 W.h/kg, significantly improves the performance and efficiency of the hybrid powertrain as more than 90% of the braking energy is regenerated.

ACKNOWLEDGMENTS

This research project was supported by MIT-Pt/EDAM-SMS/0030/2008.

REFERENCES

[1] - General Motors Corporation, BP, ExxonMobil, Shell, 2001. “Well-to-Wheel Energy Use and GHG Emissions of Advanced Fuel/Vehicle Systems”.
URL: http://www.transportation.anl.gov/pdfs/TA/163.pdf

[2] - M.A. Weiss, J.B. Heywood, A. Schafer and V.K. Natarajan, 2003. “Gauging Efficiency, Well to Wheel”, Mech. Eng. Power 2003. URL:http://www.memagazine.org /mepower03 /gauging/gauging.html

[3] URL: http://www.teslamotors.com/media/white_papers/ The21stCenturyElectricCar.pdf (last accessed on the 8th June 2009).

[4] - M.A. Weiss, J.B. Heywood et al. 2003. “Comparative Assessment of Fuel Cell Cars”, MIT, Int. Rpt. LFEE 2003-001 RP. URL:http://lfee.mit.edu/public/LFEE_2003-001_RP.pdf

[5] - K.J. Kelly, M. Zolot, G. Glinsky and A. Hieronymus, 2001. “Test Results and Modelling of the Honda Insight Using ADVISOR”, Nat. Renewable Energy Lab., Int. Rpt NREL/CP-540-31085.

[6] - “Strigear - a more efficient hybrid”, Stridsberg Powertrain AB. URL: http://www.powertrain.se/index.htm (last accessed on the 8th June 2009).

[7] - G.P. Shultz and R.J. Woosley, 2005. “The Petroleum Bomb”, Mech. Eng., Oct. 05, ASME.

[8] - The California Cars Initiative for Plug-In Hybrids. URL: http://www.calcars.org/ (last accessed on the 8th June 2009).

[9] - G.P. Shultz and R.J. Woosley, 2005. “Oil and Security”, The Committee on the Present Danger.

[10] - W.F. Milliken and D.L. Milliken 1995. “Race Car Vehicles Dynamics”, SAE International.

[11] - T.D. Gillespie, 1992. “Fundamentals of Vehicle Dynamics”, SAE International.

[12]- V. Sumatran, and G. Sovran, 1996. “Vehicle Aerodynamics”, SAE International.

[13]- J.M.O BRITO, 2007. “Modelo de Gestão de Energia de um Veículo Híbrido Eléctrico, Assistido por Motor Térmico e Travagem Regenerativa”, MSc thesis, Universidade do Minho.

[14]- A.M.D. ROCHA, 2008. “Simulação Energética de um Veículo Híbrido Plug-in em Circulação Real Suburbana”, MSc thesis, Universidade do Minho.